

Biexciton binding energy and exciton–LO-phonon scattering in ZnSe quantum wires

H. P. Wagner*

Technische Universität Chemnitz, Institut für Physik, D-09107 Chemnitz, Germany

H.-P. Tranitz and R. Schuster

Universität Regensburg, Institut für Physik II, D-93040 Regensburg, Germany

G. Bacher and A. Forchel

Technische Physik, Universität Würzburg, Am Hubland, D-97074 Würzburg, Germany

(Received 7 June 2000; revised manuscript received 7 November 2000; published 28 March 2001)

The dependence of the biexciton binding energy and of the exciton–LO-phonon scattering rate on the wire width is investigated in wet-etched ZnSe quantum wires by temperature-dependent transient four-wave mixing. We observe an increase of the biexciton binding energy with decreasing wire width, reaching an enhancement of about 30% in the smallest wire structure. In addition, we find a decrease of the exciton–LO-phonon scattering rate with decreasing wire size, which is discussed with consideration of the reduced polarity of the exciton wave function and the modified density of final states in narrow wire structures.

DOI: 10.1103/PhysRevB.63.155311

PACS number(s): 71.35.–y, 42.50.Md, 71.55.Gs

Recently, quasi-one-dimensional quantum wire (QWR) structures have attracted great attention for potential optoelectronic and all-optical device applications since they are theoretically predicted to offer superior optical and electrical properties.^{1–3} The reduced dimensionality leads to pronounced excitonic effects due to an increased electron-hole overlap modifying the binding energies of excitons^{4–7} and excitonic molecules.^{8,9} Furthermore, scattering processes with excitons^{10–13} and acoustic phonons^{13,14} are changed compared to quasi-two-dimensional quantum well (QW) systems. Some of these effects were studied on III-V QWR systems using ultrafast degenerate four-wave mixing (FWM) techniques^{8,11,12,14} while quantum wires prepared from wide-gap II-VI material are less well investigated.^{9,10} Due to their large exciton oscillator strength high biexciton binding energies and strong Fröhlich interaction, however, II-VI QWR structures are well suited to examine quantum coherent processes such as the scattering of excitons with LO phonons and the formation and binding energy of biexcitons. Both properties are so far theoretically not well described in QWR structures but are of importance for possible applications, since its modification changes the figure of merit in nonlinear optoelectronic or all-optical devices. It is therefore of interest to study the size dependence of LO-phonon scattering and the biexciton binding energy experimentally.

In this paper, we study etched ZnSe quantum wires by spectrally resolved transient FWM. The size dependence of the biexciton binding energy and of the exciton–LO-phonon interaction are investigated, and negatively charged excitons are observed using FWM. The QWR structures were processed by electron-beam lithography and wet chemical etching from a Zn_{0.9}Mg_{0.1}Se/ZnSe single quantum well (QW), which was pseudomorphically grown on (001) GaAs by molecular-beam epitaxy. The active ZnSe layer of 10 nm thickness is sandwiched between two 30-nm-thick Zn_{0.9}Mg_{0.1}Se barriers, defining a type-I QW (Ref. 15) (sample A in Ref. 17). The patterned wire arrays have sizes of 100 $\mu\text{m} \times 100 \mu\text{m}$ and comprise wires of 300 nm down to

25 nm width, which was confirmed by scanning electron microscopy. In addition to the QWR structures, unpatterned 100 $\mu\text{m} \times 100 \mu\text{m}$ mesa structures are provided on the sample as a quasi-2D reference. A detailed description of the fabrication process is given in Ref. 16.

As the excitation source for the experiments we used a frequency-doubled mode-locked Ti-sapphire laser, providing 100-fs pulses with a spectral width of 22 meV at a repetition rate of 82 MHz. The two-pulse degenerate FWM experiments were performed in reflection geometry, applying collinear polarized excitation fields. The $1/e^2$ focus diameter of the pulses on the sample was measured with a charge-coupled device (CCD) camera to 100 μm . The FWM signal was recorded in a time-integrated manner and spectrally resolved by a combination of a spectrometer and an optical multichannel analyzer as a function of the time delay τ between the two incident pulses. The samples were kept in a variable temperature helium cryostat at temperatures between $\bar{T}=20$ and 80 K.

FWM measurements were made on the QWR arrays and on the mesa structures. Normalized FWM spectra are shown in Fig. 1(a) for the mesa and QWR arrays of 55, 42, 36, 28, and 25 nm wire width at a delay time of $\tau=0.2$ ps and $\bar{T}=20$ K. In all cases, the excitation intensity was 250 nJ/cm² [corresponding to a two-dimensional (2D) exciton density of about 6×10^9 cm⁻²], and the laser center wavelength was set to the lowest excitonic transition, avoiding excitation of the excitonic continuum. A 100-fs pulse spectrum is given as the dashed line. In the etched wires, the structure undergoes an elastic relaxation perpendicular to the wire's $\langle 011 \rangle$ direction due to the free-standing side walls, which saturates for wire sizes less than 30 nm.⁷ This results in a redshift of the exciton energies in the QWR structures compared to the mesa structure.¹⁰ In the 55-nm QWR structure the X line shows an inhomogeneous broadening of about 2 meV due to strain fluctuations or surface fields. With decreasing QWR size, a blueshift of the X transition is observed [see Fig. 1(a)], which

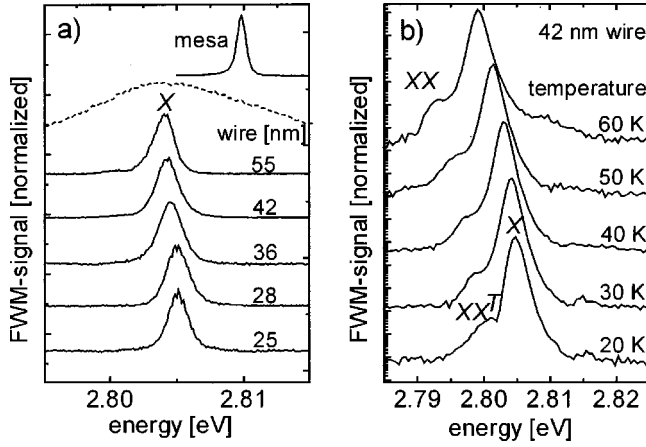


FIG. 1. (a) FWM spectra for the mesa (top) and QWR arrays of 55, 42, 36, 28, and 25 nm wire width recorded at a delay time of $\tau \approx 0.2$ ps and a lattice temperature $\bar{T} = 20$ K. The dashed curve gives the spectrum of the 100-fs pulse. (b) FWM spectra of the 42-nm-wide wire array on a logarithmic scale recorded at various lattice temperatures as labeled. X, T, and XX denote the exciton-, trion-, and biexciton-induced transitions. The excitation intensity of the two 100-fs pulses was 2.5 MW/cm^2 .

is due to the quantum wire confinement. The inhomogeneous broadening is not significantly increased for the smaller wires. Even for the smallest QWR the increase of the inhomogeneous broadening is less than 10% and thus much smaller than the quantum confinement energy, showing that the lateral size fluctuations are in all cases much less than the lateral size itself. The lateral exciton localization energy is in all cases less than the biexciton binding energy.

In addition to the X FWM peak, a weak signal is detected at the low-energy side of the X transition as shown in Fig. 1(b) for a 42-nm-wide QWR at $\bar{T} = 20$ K. The signal is attributed to the formation of biexcitons XX and trions T in correspondence with previous investigations on similar QW's.^{17,18} As in these structures we attribute the formation of trions to electrons that are photoexcited from the GaAs substrate, captured by the QWR potential and localized by the reverse electric field in the GaAs substrate. While the biexciton-induced transition XX and the trion transition T can be spectrally resolved in the unprocessed QW at low excitation intensities,¹⁷ the XX and T transitions are spectrally overlapping in the QWR structures. However, the contribution of trions can be recognized by their weak polarization interference with the exciton X signal as demonstrated in the FWM traces obtained from a 25-nm-wide wire array in Fig. 2 at low temperatures. From the beating period of $T_T = 1.5 \pm 0.4$ ps, which is similar for all QWR structures within the experimental accuracy, we can estimate a trion binding energy of $E_T = 2.8 \pm 0.6$ meV. This value is also found in the mesa and in comparable QW structures.^{17,18}

As in previous investigations on QW structures the excess electron density in the QWR structures is reduced with increasing temperature due to a thermal activation of the carriers over the $\text{Zn}_x\text{Mg}_{1-x}\text{Se}$ barrier back to the GaAs substrate. Thus a decrease of the trion transition signal is observed at higher temperatures¹⁷ [see Fig. 1(b)], leading to

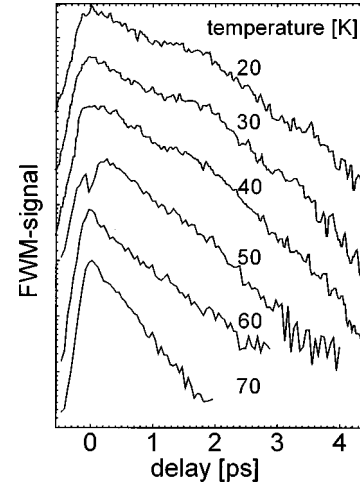


FIG. 2. FWM traces at the lowest wire subband exciton energy of the 25-nm-wide wire array recorded at various lattice temperatures as labeled. The excitation intensity was 2.5 MW/cm^2 .

a less pronounced beating structure in the FWM traces (see Fig. 2). Above 45 K the trion contribution is negligible and the biexciton-induced XX transition remains in the FWM spectrum. Hence we can isolate the XX signal from the T transition and are able to determine the biexciton binding energy E_{XX} as a function of the wire size from the energy difference between the exciton X and the XX transition as shown previously in a ZnSe QW.^{17,18} Figure 3 shows the FWM spectra of all investigated QWR structures at a delay time of $\tau = -0.2$ ps. Corresponding biexciton binding energies are given in the inset of Fig. 3, where also spectra at temperatures $\bar{T} > 45$ K were taken into account. A clear wire width dependence of the biexciton binding energy is observed, showing an energy increase from $E_{XX} = 5 \pm 0.35$ meV in the mesa structure to $E_{XX} = 6.7 \pm 0.35$ meV in

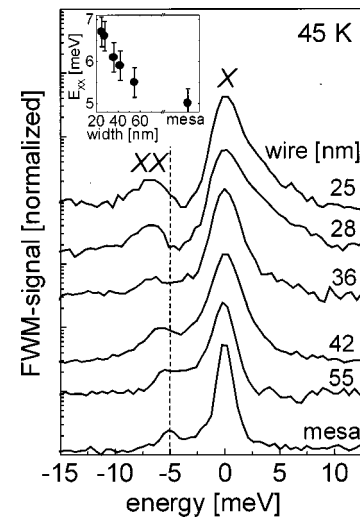


FIG. 3. FWM spectra on a logarithmic scale for the mesa (bottom) and QWR arrays of 55, 42, 36, 28, and 25 nm wire width recorded at a delay time of $\tau \approx -0.2$ ps and a lattice temperature $\bar{T} = 45$ K. The inset shows the evaluated biexciton binding energy E_{XX} as a function of the wire size.

the smallest QWR array. A similar enhancement of the biexciton binding energy has also been observed in FWM experiments on QWR structures prepared from a 20-nm $\text{Zn}_{0.9}\text{Mg}_{0.1}\text{Se}/\text{ZnSe}$ single QW structure.⁹ Since we do not expect an increase of the exciton binding energy for the investigated wires with lateral sizes equal or larger than 6 times the Bohr radius,¹⁹ the enhancement of the biexciton binding energy is not attributed to a dielectric exciton confinement but is explained by a larger biexciton wave function that is more susceptible to the confinement. The observed dependence is in agreement with a model for the biexciton binding in localized systems,²⁰ in which the ratio between the biexciton binding energy and the exciton confinement energy is the important parameter. An overview of this modeling for ZnSe QW and QWR structures is in preparation.⁹

The influence of the acoustic- and optical-phonon scattering as well as the temperature dependence of the electron/trion-exciton scattering on the exciton dephasing was investigated by temperature-dependent FWM measurements. Figure 4 shows the experimentally obtained homogeneous exciton linewidth $\Gamma_X = h/(\pi T_2)$ as a function of the lattice temperature for all investigated QWR structures and the mesa structure at an excitation density of $n_X \approx 5 \times 10^9 \text{ cm}^{-2}$. While the mesa structure was treated in the homogeneous broadening limit,¹⁷ the dephasing time T_2 in the wire structures was determined by the relation $T_2 = 4\tau_d$ (Ref. 21) (τ_d being the experimentally observed decay) since wire width fluctuations lead to an inhomogeneous broadening. A comparison with calculations by Erland *et al.*,²² who considered the increased ratio of the homogeneous to inhomogeneous broadening at higher temperatures, shows that this relation holds for whole temperature range.

The homogeneous linewidth of each structure observed at $\tilde{T} = 20 \text{ K}$ is shown in the inset of Fig. 4. We find a decrease of the homogeneous linewidth with decreasing wire size, which is attributed to a reduced electron-exciton scattering due to a trapping of electrons by surface states generated by the wire fabrication process and due to a weak exciton localization caused by fluctuations of the wire width. For a better comparison of the size dependence the linewidth curves are offset relative to each other in Fig. 4, and the homogeneous linewidth is given as linewidth change $\Delta\Gamma_X = \Gamma_X(\tilde{T}) - \Gamma_X(20 \text{ K})$ relative to the corresponding linewidth value at $\tilde{T} = 20 \text{ K}$ given in the inset of Fig. 4. The observed temperature dependence of the decay rate is described by the following relation:²³

$$\Gamma_X(\tilde{T}, n_X) = \Gamma_X(\tilde{T} = 0 \text{ K}, n_X) + \beta_{ac}(w)\tilde{T} + \frac{\beta_{LO}(w)}{\exp(E_{LO}/k_B\tilde{T}) - 1} + \gamma_X n_{e+T}(\tilde{T}), \quad (1)$$

where $\beta_{ac}(w)$ and $\beta_{LO}(w)$ are the acoustic- and optical-phonon scattering parameters that are dependent on the wire width w , $E_{LO} = 31.6 \text{ meV}$ is the longitudinal-optical-phonon energy, k_B is the Boltzmann constant, and $\Gamma_X(\tilde{T} = 0 \text{ K}, n_X)$ is the low-temperature homogeneous linewidth. The last term in Eq. (1) considers the broadening due to the electron/trion-

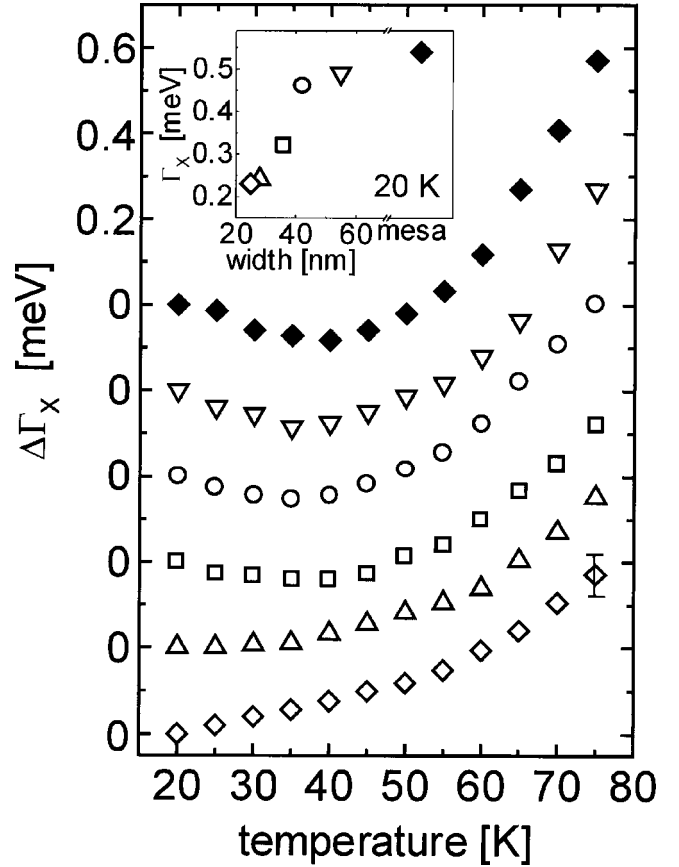


FIG. 4. Change of the homogeneous linewidth $\Delta\Gamma_X$ as a function of the lattice temperature \tilde{T} for the 55, 42, 36, 28, and 25 nm QWR arrays and the mesa structure. The curves are offset relative to each other for better comparison. The inset shows the homogeneous linewidth Γ_X of all structures at a lattice temperature of $\tilde{T} = 20 \text{ K}$.

exciton scattering γ_X with $n_{e+T}(\tilde{T})$ being the temperature-dependent density of electrons and trions in the QWR.¹⁸

The observed temperature dependence of the decay rate exhibits two different regimes. Below 40 K, the decay rates decrease with increasing temperature in wires above 28 nm wire size and in the quasi-2D mesa structure. As already mentioned the equilibrium carrier concentration $n_{e+T}(\tilde{T})$ decreases with increasing temperature, due to a thermal activation of the electrons from the confinement potential.^{17,18} This decrease leads to a reduction of the electron/trion-exciton scattering rate, which overcompensates the increase of the linewidth Γ_X due to acoustic-phonon-exciton scattering. In contrast we find a slight increase of the homogeneous linewidth Γ_X with increasing temperature for the 28- and 25-nm-wide QWR structures. In these structures both a reduction of the electron/trion-exciton scattering rate due to exciton localization or electron pinning at the quantum-wire surface and an increase of the acoustic scattering parameter $\beta_{ac}(w)$ due to the increased wire confinement can explain the observed increase of Γ_X .

At temperatures above 40 K the captured carrier density is so low that the trion T FWM signal and the polarization interference in the X FWM trace is no longer observable but

Γ_X further increases due to the onset of exciton–LO-phonon scattering. In the mesa structure the LO-phonon scattering parameter takes the value of $\beta_{LO}=70\pm 5$ meV obtained from a fit using Eq. (1) where a 2D acoustic-phonon–exciton parameter of $\beta_{ac}=4$ $\mu\text{eV/K}$ was used.²⁴ The obtained value of β_{LO} is in fair agreement with previous investigations on similar ZnSe QW structures.²⁵ In the QWR structures the LO-phonon scattering parameter $\beta_{LO}(w)$ decreases with decreasing wire size. A rough estimate using Eq. (1) and a constant acoustic-phonon–exciton parameter of $\beta_{ac}=4$ $\mu\text{eV/K}$ for all wires give the values of $\beta_{LO}(w)=55, 45, 40, 30,$ and 25 meV for the wire sizes $w=55, 42, 36, 28,$ and 25 nm, respectively. Since there is to our knowledge no theoretical model treating the optical-phonon scattering parameter $\beta_{LO}(w)$ in quantum wires as a function of the wire size we propose the following qualitative arguments to explain the observed behavior.

The lateral confinement of electrons and holes perpendicular to the wire direction that is provided by the vacuum/ZnSe interface can be modeled by an infinite barrier. Along this direction the electron and hole wave functions are identical. With decreasing wire width the polarity of the carrier (electron-hole) distribution is thus reduced, leading to a reduced polar intraband Fröhlich interaction of LO phonons.²⁶

Furthermore, the LO-phonon–exciton scattering rate is influenced by the density of final states, which are higher exciton subband states and continua. Since the energy differences of the subband states increase with decreasing wire

size the density of final scattering states within the range of the LO-phonon energy can be reduced in narrow wires.¹⁴

In conclusion we have investigated ZnSe QWR structures etched from a $\text{Zn}_{0.9}\text{Mg}_{0.1}\text{Se}/\text{ZnSe}$ single QW by spectrally resolved degenerate FWM. Temperature-dependent measurements isolate the biexciton-induced signal XX from a trion T transition, which is due to electrons that are photoexcited from the GaAs substrate and captured by the QWR potential. The biexciton binding energy E_{XX} increases with decreasing wire size up to 30% in the smallest wire compared to the QW value of $E_{XX}=5.0$ meV. The enhancement of E_{XX} is attributed to the confinement of the relatively large biexciton wave function in the QWR. Temperature-dependent measurements show a decrease of the exciton–LO-phonon scattering rate $\beta_{LO}(w)$ with decreasing wire size. The decrease of $\beta_{LO}(w)$ is tentatively explained by a reduced polarity of the exciton wave function due to the wire confinement and due to a reduced number of final subband states that can be reached within the LO-phonon energy. The experimentally observed reduced LO-phonon scattering and increased biexciton binding energy in small QWR structures are advantageous for the use of nonlinear optical applications and motivate the need for a theoretical explanation.

We thank H. Preis for providing the $\text{Zn}_{0.9}\text{Mg}_{0.1}\text{Se}/\text{ZnSe}$ single QW structure. Stimulating discussions with W. Langbein and T. L. Reinecke are kindly acknowledged. This work was supported by the Deutsche Forschungsgemeinschaft.

*Author to whom correspondence should be addressed. Email address: hp.wagner@physik.tu-chemnitz.de

¹Y. Arakawa and H. Sakaki, *Appl. Phys. Lett.* **40**, 939 (1982).

²H. Temkin, G. J. Dolan, M. B. Panish, and S. N. G. Chu, *Appl. Phys. Lett.* **50**, 413 (1987).

³Y. Z. Hu, M. Lindberg, and S. W. Koch, *Phys. Rev. B* **42**, 1713 (1990).

⁴W. Langbein, H. Gislason, and J. M. Hvam, *Phys. Rev. B* **54**, 14 595 (1996).

⁵M. Grundmann, O. Stier, A. Schliwa, and D. Bimberg, *Phys. Rev. B* **61**, 1744 (2000).

⁶M. Bayer, S. N. Walck, T. L. Reinecke, and A. Forchel, *Phys. Rev. B* **57**, 6584 (1998).

⁷T. Kummell, G. Bacher, A. Forchel, G. Lermann, W. Kiefer, B. Jobst, D. Hommel, and G. Landwehr, *Phys. Rev. B* **57**, 15 439 (1998).

⁸T. Baars, W. Braun, M. Bayer, and A. Forchel, *Phys. Rev. B* **58**, R1750 (1998).

⁹H. P. Wagner, H.-P. Tranitz, W. Langbein, J. M. Hvam, G. Bacher, and A. Forchel (unpublished).

¹⁰H. P. Wagner, W. Langbein, J. M. Hvam, G. Bacher, T. Kummell, and A. Forchel, *Phys. Rev. B* **57**, 1797 (1998).

¹¹W. Braun, M. Bayer, A. Forchel, O. M. Schmitt, L. Banyai, H. Haug, and A. I. Filin, *Phys. Rev. B* **57**, 12 364 (1998).

¹²W. Langbein, H. Gislason, and J. M. Hvam, *Phys. Rev. B* **60**, 16 667 (1999).

¹³Rajesh Kumar, A. S. Vengurlekar, A. Venu Gopal, T. Melin, F. Laruelle, B. Etienne, and J. Shah, *Phys. Rev. Lett.* **81**, 2578

(1998).

¹⁴W. Braum, M. Bayer, A. Forchel, H. Zull, J. P. Reithmaier, A. I. Filin, and T. L. Reinecke, *Phys. Rev. B* **56**, 12 096 (1997).

¹⁵M. Würz, E. Griehl, Th. Reisinger, B. Flierl, D. Haserer, T. Semmler, T. Frey, and W. Gebhardt, *Phys. Status Solidi B* **202**, 805 (1997).

¹⁶M. Illing, G. Bacher, T. Kummell, A. Forchel, T. G. Anderson, D. Hommel, D. Jobst, and G. Landwehr, *Appl. Phys. Lett.* **67**, 124 (1995).

¹⁷H. P. Wagner, H.-P. Tranitz, and R. Schuster, *Phys. Rev. B* **60**, 15 542 (1999).

¹⁸H. P. Wagner, H.-P. Tranitz, and R. Schuster, *Phys. Status Solidi B* **221**, 499 (2000).

¹⁹M. Bayer, S. N. Walck, T. L. Reinecke, and A. Forchel, *Phys. Rev. B* **57**, 6584 (1998).

²⁰W. Langbein and J. M. Hvam, *Phys. Rev. B* **59**, 15 405 (1999).

²¹T. Yajima and Y. Taira, *J. Phys. Soc. Jpn.* **47**, 1620 (1979).

²²J. Erland, K.-H. Pantke, V. Mizeikis, V. G. Lyssenko, and J. M. Hvam, *Phys. Rev. B* **50**, 15 047 (1994).

²³S. Rudin, T. L. Reinecke, and B. Segall, *Phys. Rev. B* **42**, 11 218 (1990).

²⁴A. J. Fischer, D. S. Kim, J. Hays, W. Sham, J. J. Song, D. B. Eason, J. Ren, J. F. Shetzina, H. Luo, J. K. Furdyna, Z. Q. Zhu, T. Yao, J. F. Kiem, and W. Schäfer, *Phys. Rev. Lett.* **73**, 2368 (1994).

²⁵H. P. Wagner, A. Schätz, R. Maier, W. Langbein, and J. M. Hvam, *Phys. Rev. B* **57**, 1791 (1998).

²⁶Y. Toyozawa, *Prog. Theor. Phys.* **12**, 111 (1959).